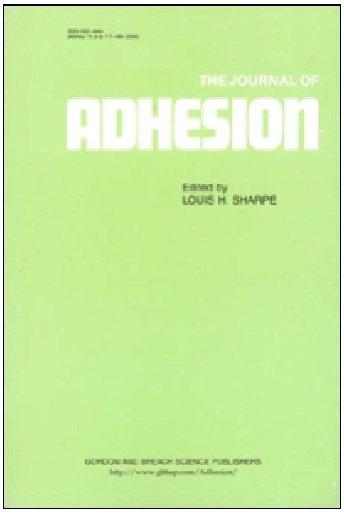

The Journal of Adhesion
Publication details, including instructions for authors and subscription information:
http://www.informaworld.com/smpp/title~content=t713453635

Dynamic Contact Angles of Viscous Liquids

Dennis G. Welygan[ab]; Charles M. Burns[a]
[a] Department of Chemical Engineering, University of Waterloo, Waterloo, Ontario, Canada [b] BS & CP Laboratory, 3M company, St. Paul, Minnesota

To cite this Article Welygan, Dennis G. and Burns, Charles M.(1980) 'Dynamic Contact Angles of Viscous Liquids', The Journal of Adhesion, 11: 1, 41 — 55
To link to this Article: DOI: 10.1080/00218468008078903
URL: http://dx.doi.org/10.1080/00218468008078903

J. Adhesion, 1980, Vol. 11, pp. 41–55
0021-8464/80/1101-0041 $04.50/0

Printed in Great Britain

Dynamic Contact Angles of Viscous Liquids

DENNIS G. WELYGAN† and CHARLES M. BURNS
Department of Chemical Engineering, University of Waterloo, Waterloo, Ontario, Canada, N2L 3G1

(*Received February 14, 1978; in final form February 10, 1980*)

An empirical model has been developed which can predict the dynamic contact angle of a spreading drop of viscous liquid on a plane wettable surface from the contact area for contact angles between 90° and 0° within a specified drop size. This range of drop size is restricted to those drops having a contact area at a 90° cap condition (A_{90}) between 0.10 cm^2 and 0.20 cm^2 The drop profile was found not to be that of a spherical segment and hence could not allow a simple geometric interpretation. The model strengthens the interpretation that contact angle development in this range of drop size is mainly the geometric result of spreading. The model was found to hold over a wide variety of polymer melt temperatures (155–240°C), molecular weights and molecular weight distributions, which combined would greatly influence drop profile. The time dependency of the dynamic contact angle was also evaluated by combining the present empirical model with a previous viscosity dependent model relating contact area with time. The model was successfully applied to the unrelated systems of silicone oil and glycerol at room temperature indicating its general applicability.

INTRODUCTION

The relationship of an equilibrium contact angle for a sessile drop resting on a plane solid surface with the relevant surface properties is well known from Young's equation,

$$\gamma_{SV} - \gamma_{SL} = \gamma_{LV} \cos \theta_e \tag{1}$$

where γ_{SV} is the solid-vapour interfacial energy,
γ_{SL} is the solid-liquid interfacial energy,
γ_{LV} is the liquid-vapour interfacial energy, and
θ_e is the equilibrium contact angle.

Also, the shape of sessile drops at equilibrium under the influence of both surface tension and gravity may be calculated from the tables of Bashforth

---

† Present address: BS & CP Laboratory, 3M company, 251-3, St. Paul, Minnesota 55101.

and Adams.[1] The current study is directed towards the less well-defined, nonequilibrium or dynamic contact angle situation. The ability to predict the dynamic contact angle of a spreading sessile drop has not yet been completely resolved. Some examinations of wetting kinetics have attempted to relate spreading velocity directly[2] to dynamic contact angle whereas others required that dynamic contact angle be considered as a measure of the driving force necessary for wetting. There is a variety of models in the literature[2–7] which attempt to describe wetting kinetics with various degrees of success. This study will show that the applicability of four of these models to the present data is inadequate and that an empirical technique, with parameters obtained from analysis of viscous drop profiles, provides an alternative description of dynamic contact angles.

Drop geometry is fundamental to the study of dynamic contact angle. The spreading sessile drop has been likened to a spreading segment of a spheroid and hence the majority of the current spreading models incorporates this spherical segment approach. Indeed, Schonhorn[3] presented data for the system Elvax 220 on aluminium which showed that the radius r of the drop was a universal function of the contact angle θ, closely approximated by:

$$\frac{r^3}{V} = 3/\pi \left[\frac{\sin\theta\,(1+\cos\theta)}{(1-\cos\theta)(2+\cos\theta)} \right] \tag{2}$$

which follows from the geometry of a spherical segment. V is the constant volume of the spreading drop.

A number of authors have reported that the drop profiles for certain viscous systems, however, could not be represented by a spherical segment approximation. Arslanov[6] for instance showed that by treating the spreading drop as a cone, he could obtain better agreement. Lau[8] observed that the spreading profiles were not those of a spherical segment, noting that perhaps a cycloidal shape seemed more likely, but he could find no simple analytic solution. The consensus appears that the spherical segment approximation may be valid for low viscosity liquids, but for very viscous melts, the spherical segment approximation is generally invalid.

Ryley and Khoshaim[9] have recently shown that the static contact angle may be calculated by assuming the drop profile to be a section of an ellipse or that the spreading drop is a segment of an oblate spheroid.

Newman[2] suggested that the contact angle could be directly related to time through the relationship

$$\cos\theta_t = (\cos\theta_\infty)(1-ae^{-ct}) \tag{3}$$

where a and c were empirical constants.

With such a variety of spreading models and drop profiles the present study was directed to the examination of the spreading of viscous polymer drops in an attempt to characterize better the case of viscous spreading. The concern for drop profile is important and not trivial. Drop geometry is fundamental to a complete understanding of the spreading phenomenon because it is the response of the material to the applied forces. Hence shape must be considered in comparing model systems of spreading viscous liquids.

MATERIALS AND PROCEDURES

The polymer melts examined in this study were polystyrenes of varying molecular weight and molecular weight distribution. The molecular weights ranged from a $\bar{M}_n$ of 10,000 to 37,000 for polystyrene of narrow molecular weight distribution and from a $\bar{M}_n$ of 8,800 to a $\bar{M}_n$ of 32,000 for polystyrenes of broad molecular weight distribution. Characterization data for these polymers have been mentioned earlier.[10] The spreading rates and drop profiles were recorded on 35 mm photographic film over a temperature range of 155–240°C. Dimensions of the drops were measured with a precision of ± 0.0002 cm and contact angles to the normal $\pm 2°$. Details of polymer preparation, drop formation, temperature control and analysis have been mentioned elsewhere.[10,11]

For comparative purposes silicone oil and glycerol were also examined as they provided examples of spreading of viscous liquids other than polymer melts.

RESULTS AND DISCUSSION

In agreement with previous work[8] done in this laboratory, the drop profiles of the spreading drops were found not to be those of spherical segments. This result is better seen in Figure 1 where a comparison of measured and calculated drop radii is made using the spherical segment model suggested by Schonhorn. The deviations observed are significantly greater than any error in measurement of drop mass, melt density, drop dimension or contact angle.

Similarly, testing Newman's model of contact angle development with time for PS 8,879 at two different temperatures showed significant deviation from linearity as can be seen in Figure 2.

Arslanov's conical interpretation also left much to be desired as the contact angles calculated from the contact areas were significantly different from the contact angles measured.

An explicit empirical formula for the time dependence of cos θ has also

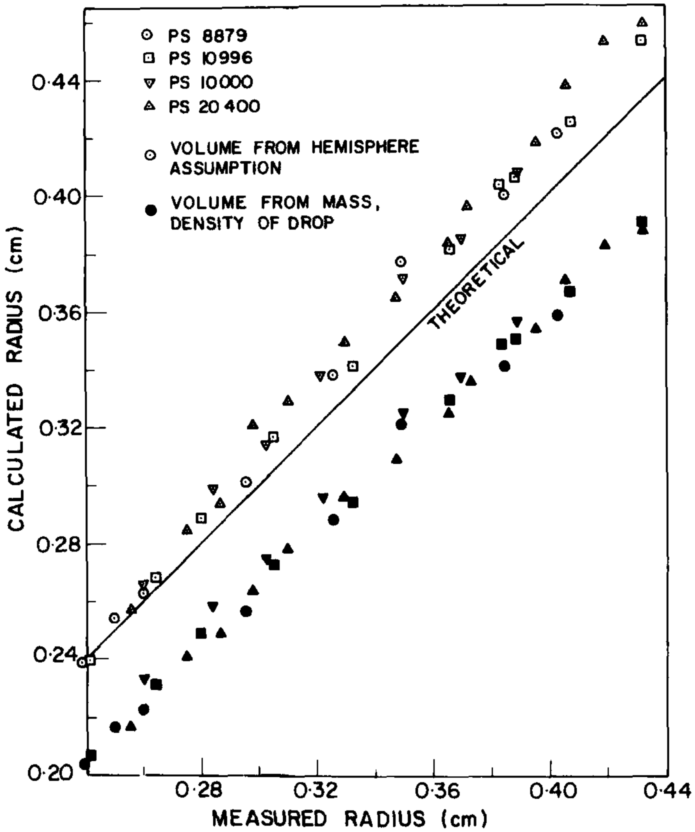

FIGURE 1 Comparison of measured and calculated drop radii using Schonhorn's spherical model (Ref. 2) for various polymers at 200°C. The solid line represents perfect agreement between calculated and measured radii. The open symbols are for radii calculated from volumes based on the hemisphere assumption. The closed symbols are for radii calculated from volumes based on the known mass and density of the drop.

been suggested by Kwei, Schonhorn and Frisch[12] and is of the form

$$\frac{\cos\theta}{\cos\theta_\infty} = \frac{kt}{1+kt} \tag{4}$$

Application of this formula to the present data results in significant deviation from linearity especially at low temperatures or high viscosity conditions. This result is shown in Figure 3. Consistent systematic deviations in fit were observed which suggest a sinusoidal nature to the curve rather than a linear fit. These results are also in agreement with VanOene, Chang and Newman[13] who observed a similar disappointing fit and led to their conclusion that the formula was best regarded as strictly empirical.

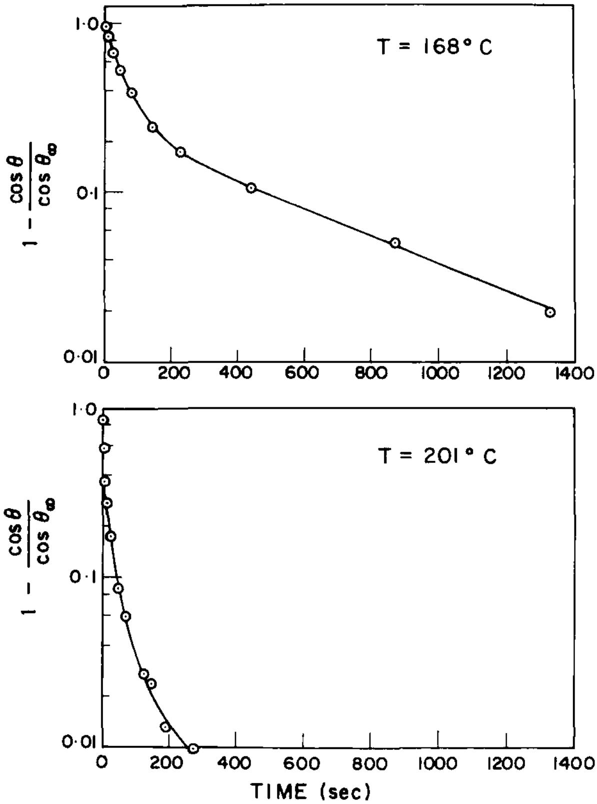

FIGURE 2 Test of Newman's model of contact angle development with time (Ref. 2) for PS 8,879 at 168° and 201°C.

With such poor agreement of the models with the actual spreading data observed, a new analysis of the data resulted in an empirical model for spreading which we will show can describe dynamic contact angle development for viscous fluids better than the current models.

An examination of Lau's[8] data suggested that a direct relationship involving the contact angle θ and contact area A for the spreading drop could be made. It was observed that often, for drops of equal spreading area, the contact angles were similar, regardless of melt temperature and molecular weight. Initially the model

$$\theta = \frac{180}{1+kA} \tag{5}$$

was suggested to account for contact angles at the extremes of small and large contact areas. The parameter k was found experimentally to vary

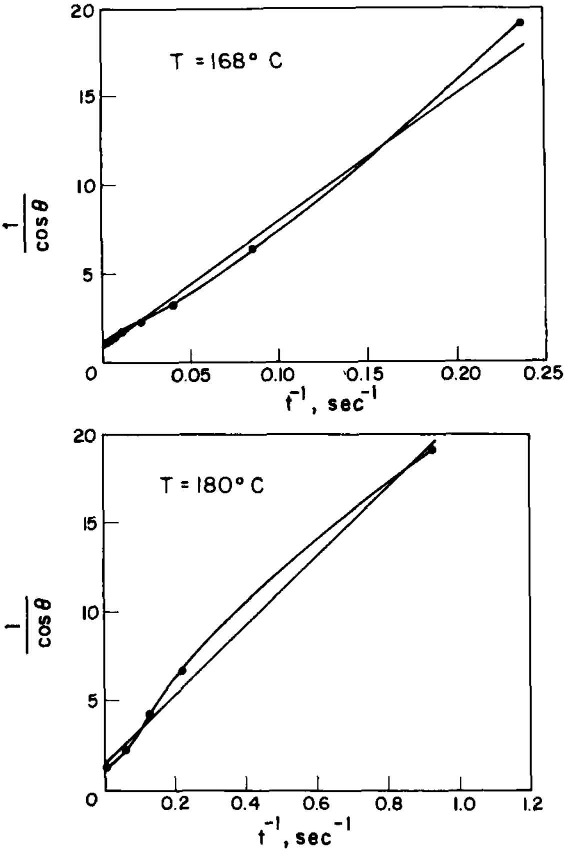

FIGURE 3 Test of Kwei, Schonhorn and Frisch's model of contact angle development with time (Ref. 12) for PS 8,879 at 168° and 180°C.

linearly with area, as can be seen in Figure 4. Using $k = mA+b$ led to the following second order function relating dynamic contact angle with area.

$$\theta = \frac{180}{1+bA+mA^2} \tag{6}$$

A sample of the experimental data necessary to calculate these parameters is shown in Table I along with a comparison of the contact angles calculated by Eq. (6) with the original contact angles. The parameters m and b were subsequently found to vary with the size of the drop and so were correlated with the area of the spreading drop at the 90° dynamic contact angle condition (normally designated A_{90}). This result is illustrated in Figures 5 and 6 for the range of drop sizes considered. This variation is to be expected as a

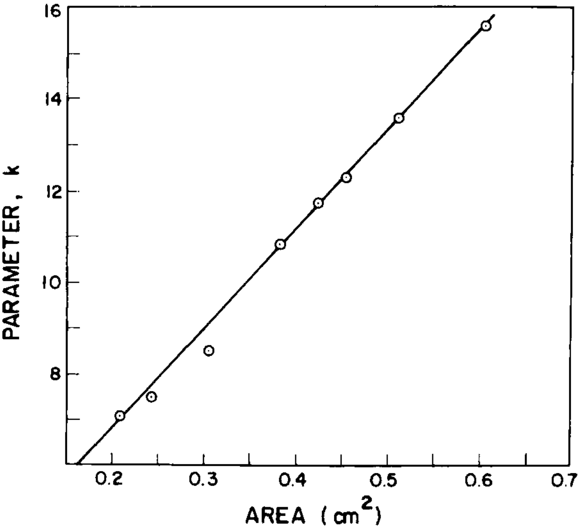

FIGURE 4 Change in parameter "k" with area for PS 10,000 at 213°C.

large drop volume and a small drop volume will at some time exhibit equal spreading areas but their contact angles will be quite different. That the same type of relationship can describe these two drops is the important point when considering the variation in drop sizes and drop spreading times.

TABLE I

Evaluation of the parameters m and b for the empirical model and comparison of the predicted contact angles for PS 10,000 at 213°C with the measured contact angles

Time (sec)	Area (cm^2)	θ_L (deg)	θ_R (deg)	$k = \left(\frac{180}{\theta} - 1\right)/\theta$	θ_{calc}
0.0	0.16359	90	90	—	—
0.93	0.20876	73	73	7.021	74.27
1.89	0.24218	64	63	7.484	63.68
4.80	0.30633	50	50	8.487	48.19
11.86	0.38350	35	35	10.802	35.54
18.17	0.42697	30	30.5	11.710	30.37
25.86	0.46337	27	26.5	12.228	26.82
39.51	0.51589	22.5	23	13.568	22.66
94.32	0.61671	17	16.5	15.547	16.91

θ_L, θ_R are the dynamic contact angles measured from the photographs at the left and right sides of the profile respectively.

$$k = mA + b$$

or $k = 21.618A + 2.306$ from above data.

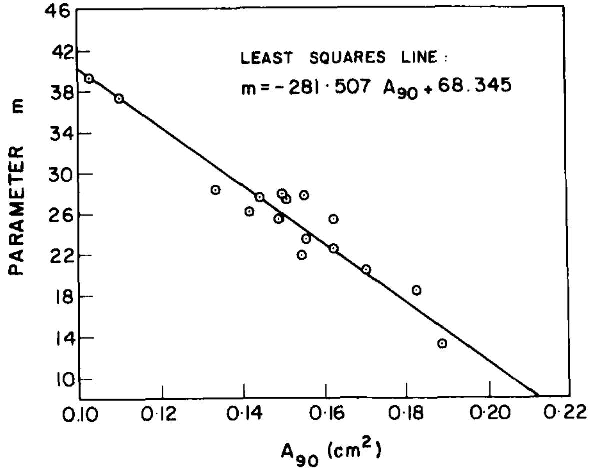

FIGURE 5 Change in parameter "m" with A_{90}.

From a least squares analysis of the experimental data the following set of parameter equations was obtained:

$$m = -281.507\,A_{90}+68.345 \tag{7}$$

$$b = -28.486\,A_{90}+7.176 \tag{8}$$

for $0.10\ \text{cm}^2 < A_{90} < 0.20\ \text{cm}^2$.

These results then allowed the contact angle to be calculated for a spreading drop whose size is within the limits specified above.

This method of analysis emphasizes that the contact angle is the necessary result of the degree of wetting of the sessile drop. That is to say, for a given drop size the contact angle is related to the specific degree of spreading of

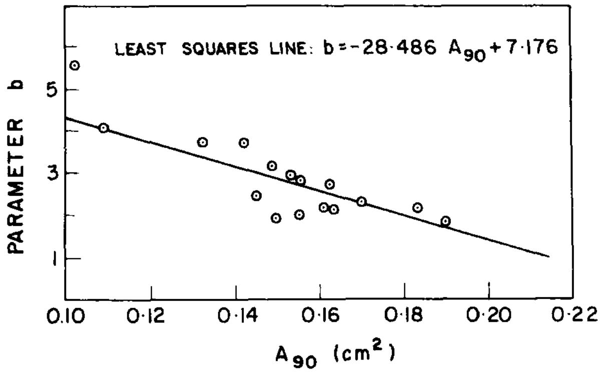

FIGURE 6 Change in parameter "b" with A_{90}.

TABLE II

Comparison of measured and empirically calculated contact angles for Lau's data[8] of PS 10,000 at 178.8° and PS 20,400 at 179°C

Area (cm^2)	L	R	θ_{calc} (deg)	
		PS 10,000 $\theta_{measured}$ (deg)		
0.2002	87	88	89.5	$A_{90} = 0.1864$
0.2085	84	85.5	86.6	$m = 15.872$
0.2181	82	83	83.3	$b = 1.866$
0.2286	80	80	79.8	
0.2374	78	76	77.0	
0.2509	74.5	73	72.9	
0.2648	72	70	69.0	
0.2771	67	68.5	65.8	
0.2868	65	65.5	63.4	
0.2966	62.5	64	61.0	
0.3355	56	54.5	52.7	
		PS 20,400		
0.1960	88	87.5	89.8	$A_{90} = 0.1847$
0.2077	85	84	85.6	$m = 16.351$
0.2167	81.5	82	82.5	$b = 1.915$
0.2328	77	78	77.2	
0.2455	74	73	73.3	
0.2606	69	69	68.9	
0.2781	65	65	64.4	

the drop at the time at which it was measured. The dynamic contact angle is the geometric necessity arising from wetting kinetics and as such is not the time dependent variable. This result is in contrast to the wetting models of Newman and Kwei, Schonhorn and Frisch, which correlate dynamic contact angle with time and imply that surface forces control the rate of spreading. In our earlier paper[10] we show that in spreading, well-wetting systems the rate of spreading is controlled simply by the viscous resistance of the fluid to the gravitational forces.

The present model was applied to some of Lau's previous data on wetting. The results are shown in Table II; these results were typical for drop sizes within the range for which the parameters were evaluated. For larger drops significant deviations were observed; it may be construed however that the drops were subjected to gravitational distortion[3] $(l_0 > (2\gamma/\rho g)^{\frac{1}{2}})$.

If the dynamic contact angle was a geometric necessity of wetting then in principle the previous equations should be applicable to other systems where the time dependency is not stressed. The present model was then

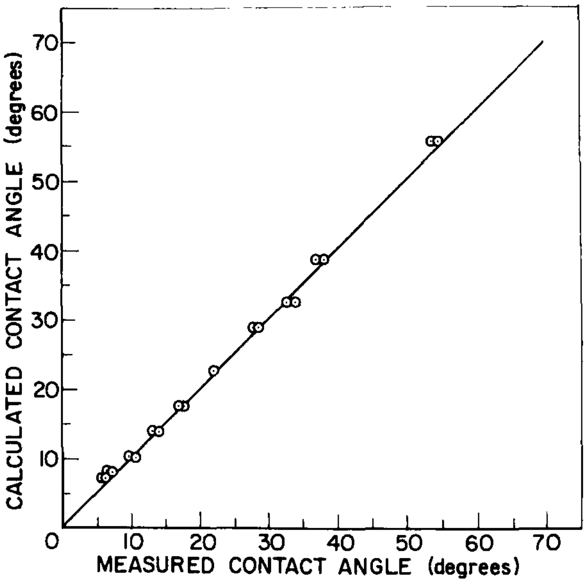

FIGURE 7 Comparison of calculated and measured contact angle for silicone oil.

applied to the spreading of silicone oil and glycerol. A comparison of contact angles calculated by Eq. (6) with the measured contact angle is shown in Figures 7 and 8 for silicone oil and glycerol respectively. The quantitative agreement is excellent.

It is also possible to show the time dependency of the dynamic contact angle by combining the present contact angle model with a contact area-time model which has been developed in our earlier paper.[10] Accordingly the dynamic contact angle can now be described as a function of time directly, with temperature and molecular weight of the polymer melt being the controlling rate parameters. The results of these combined models can be seen in Figures 9, 10 and 11 for a number of polystyrenes at a variety of temperatures. Again the agreement between the calculated curve and the actual data is excellent. The applicability of this model to viscous spreading systems appears promising.

The present contact angle model can be shown to be consistent with the spherical model but only over a limited contact angle range. For the present model the necessary parameters were obtained experimentally but the results suggest that such parameters should be a universal function for any drop and should only be related geometrically. Using Schonhorn's expression relating the contact angle and drop radius, Eqs. (2) and (5), it is possible to calculate the present parameter "*k*" for the spreading drop on such a strictly

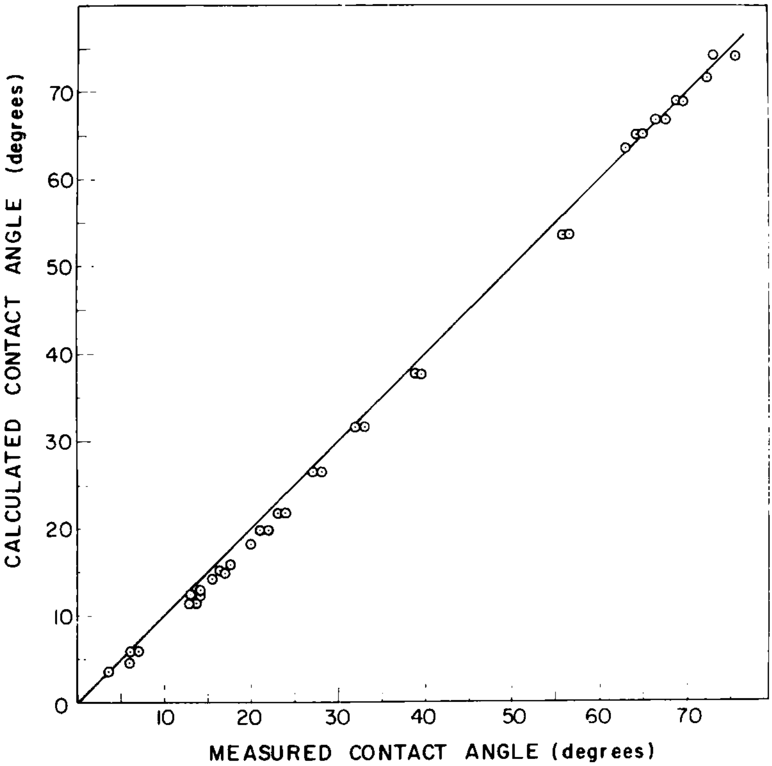

FIGURE 8 Comparison of calculated and measured contact angles for glycerol.

geometric basis, that is

$$k = \frac{(180/\theta - 1)}{\pi\left[\frac{3V}{\pi}\left(\frac{\sin\theta\,(1+\cos\theta)}{(2+\cos\theta)(1-\cos\theta)}\right)\right]^{\frac{2}{3}}} \tag{9}$$

Equation (9) can be numerically evaluated for a series of drop volumes covering the present range of interest. The resulting curves can be seen in Figure 12. The relationship involving k and Area, for true spherical spreading, is obviously different from that obtained in the present study (if compared say to Figure 4). However, over the range for which the majority of the calculations were made ($20° < \theta_d < 90°$), k may be represented as a linear function of area and as such be consistent with the present model. However, the superiority of the present empirical model can be illustrated by comparing the present empirical model for spreading as calculated by Eq. (6) with Schonhorn's spherical segment model in the form of Eq. (9) and the actual spreading curve for a given system. This comparison is shown

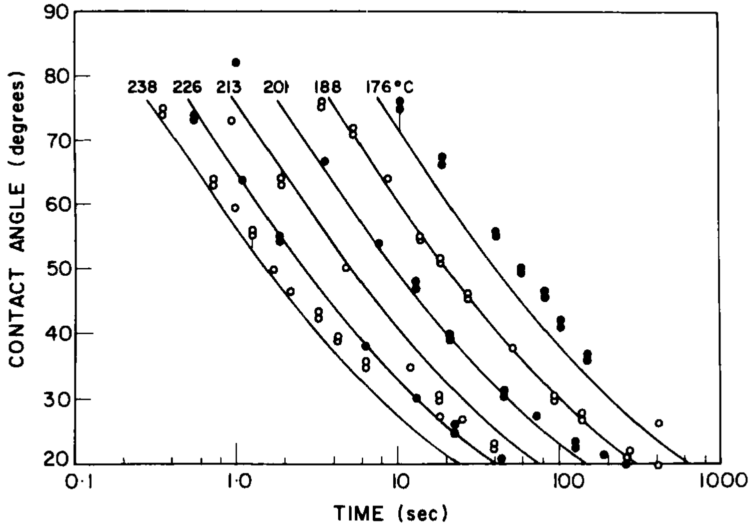

FIGURE 9 Comparison of calculated and measured dynamic contact angles for PS 10,000 at various temperatures. The calculated angles are represented by the solid lines while the measured angles are represented by the data points which are represented as open or closed alternately only for clarity.

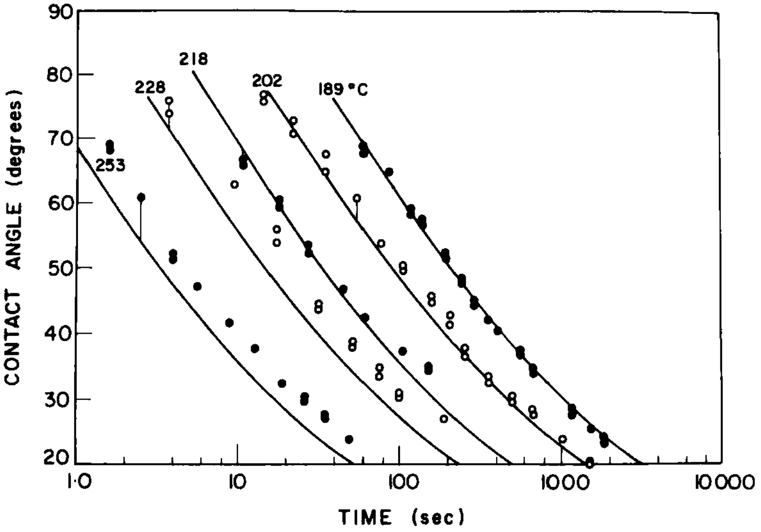

FIGURE 10 Comparison of calculated and measured dynamic contact angles for PS 37,000 at various temperatures. The calculated angles are represented by the solid lines while the measured angles are represented by the data points which are represented as open or closed alternately only for clarity.

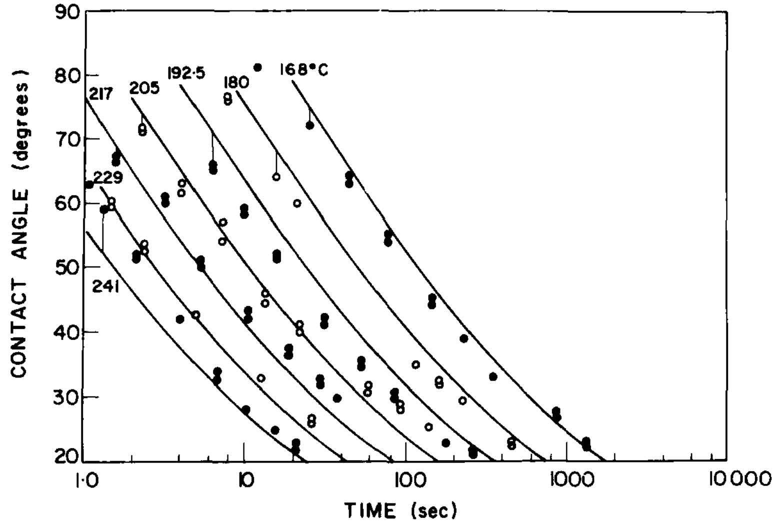

FIGURE 11 Comparison of calculated and measured dynamic contact angles for PS 8,879 at various temperatures. The calculated angles are represented by the solid lines while the measured angles are represented by the data points which are represented as open or closed only for clarity.

in Figure 13. The data further substantiate the conclusion that viscous spreading drops are different from drops of liquids of low viscosity especially for nonspherical drop profiles and at the present time an empirical relationship appears better suited to dynamic contact angle calculations. A precise geometric interpretation is still lacking.

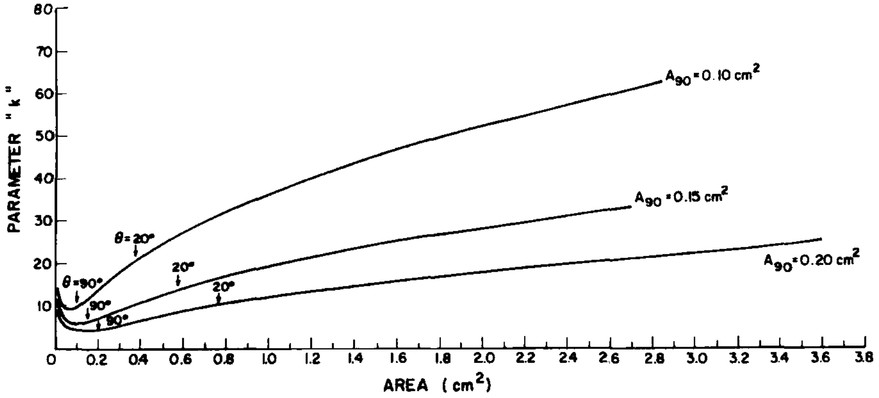

FIGURE 12 Plot of the theoretical value of "k" at various drop sizes and contact areas, assuming the spreading drop is a spherical segment.

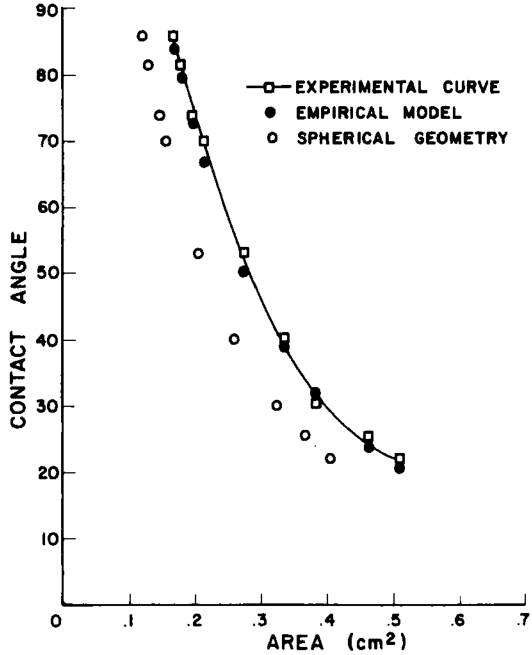

FIGURE 13 Relationship between the dynamic contact angle and the contact area as found by experimental observation (—), the present semi-empirical model (●), and the spherical segment model (○), for PS 8,879 at 200°C.

SUMMARY AND CONCLUSIONS

The spreading profiles of sessile drops of viscous polystyrene melts were observed to be not those of spherical segments. Drop profiles of low viscosity fluids have been reported to be of spherical shape and hence this difference generally supports the premise that fluid viscosity affects the drop profile within certain domains. The shape appears to approximate that of an oblate spheroid. No exact geometric description was attempted, rather the contact angle was correlated to contact area in the form of the model $\theta = 180/(1+bA+mA^2)$.

The parameters m and b were related to the size of the drop at the 90° dynamic contact angle condition. This model has been shown to describe contact angle development for a number of polystyrenes of differing molecular weights and molecular weight distributions over a wide temperature range (155–240°C). The model was successfully applied to the data of Lau and also to the unrelated systems of silicone oil and glycerol at 23°C. In combination with the previously developed model relating contact area and time, the dynamic contact angle development with time could be predicted. Satisfactory agreement was obtained over a broad range of experimental conditions. The general usefulness of such a specific correlation in its application to nonpolymer systems supports the present empirical model as a practical method of predicting contact angle development when drop size becomes a limiting criterion. At present, no theoretical model exists for prediction of dynamic contact angle development.

Acknowledgement

The authors gratefully acknowledge partial support for this research from the Defence Research Board of Canada (grant no. 7540-01) and from the National Research Council of Canada (grant no. A4511).

References

1. F. Bashforth and J. C. Adams, "An attempt to test the theories of capillary action", University Press, Cambridge, England, 1883.
2. S. Newman, *J. Colloid Interface Sci.* **26**, 209 (1968).
3. H. Schonhorn, H. L. Frisch and T. K. Kwei, *J. Applied Phys.* **37**, 4697 (1966).
4. W. E. Cherry and C. M. Holmes, *J. Colloid Interface Sci.* **29**, 174 (1969).
5. T. P. Yin, *J. Phys. Chem.* **73**, 2413 (1969).
6. V. V. Arslanov, T. I. Ivanova and V. A. Ogarev, *Dokl. Acad. Nauk. SSR*, **198**, 113 (1971).
7. W. W. Y. Lau and C. M. Burns, *J. Polym. Sci.: Polym. Phys.* **12**, 431 (1974).
8. W. W. Y. Lau, Ph.D. Thesis, University of Waterloo, 1973.
9. D. J. Ryley and B. H. Khoshaim, *J. Colloid Interface Sci.* **59**, 243 (1977).
10. D. G. Welygan and C. M. Burns, *J. Adhesion* **10**, 123 (1979).
11. D. G. Welygan, Ph.D. Thesis, University of Waterloo, 1977.
12. T. K. Kwei, H. Schonhorn and H. L. Frisch, *J. Colloid Interface Sci.* **28**, 543 (1968).
13. H. VanOene, Y. F. Chang and S. Newman, *J. Adhesion* **1**, 54 (1969).